Curvature perturbation spectra from waterfall transition, black hole constraints and non-Gaussianity

Edgar Bugaev* and Peter Klimai†
Institute for Nuclear Research, Russian Academy of Sciences, 60th October Anniversary Prospect 7a, 117312 Moscow, Russia

We carried out numerical calculations of a contribution of the waterfall field to the primordial curvature perturbation (on uniform density hypersurfaces) ζ, which is produced during waterfall transition in hybrid inflation scenario. The calculation is performed for a broad interval of values of the model parameters. We show that there is a strong growth of amplitudes of the curvature perturbation spectrum in the limit when the bare mass-squared of the waterfall field becomes comparable with the square of Hubble parameter. We show that in this limit the primordial black hole constraints on the curvature perturbations must be taken into account. It is shown that, in the same limit, peak values of the curvature perturbation spectra are far beyond horizon, and the spectra are strongly non-Gaussian.

PACS numbers: 98.80.-k

I. INTRODUCTION

In last two years an interest in hybrid inflation models was very much revived [1–7]. The main questions which were discussed are dynamics of the waterfall field and its influence on the total spectrum of density perturbations produced by inflationary expansion. It was suggested, in particular, that fluctuations in the waterfall field could lead to non-Gaussian curvature perturbation at rather large scales (even, possibly, at cosmological scales). Note that, in general, hybrid inflation models remain theoretically attractive up to now, especially in the context of supergravity and string theories (see, e.g., [8, 9]).

In many cosmological scenarios the period just after the end of inflation, i.e., the inflaton decay and the subsequent evolution of the decay products to a thermal equilibrium starts with preheating, and one of the most studied models is hybrid inflation with tachyonic preheating. It had been shown in [10] that preheating after hybrid inflation goes through the tachyonic amplification due to the dynamical symmetry breaking, when one of the fields rolls to the minimum through the region where its effective mass-squared is negative. In the process of this rolling amplitudes of field fluctuations grow exponentially leading to a fast decrease of a height of the inflationary potential ("false vacuum decay").

As is shown in the recent papers [1–7] the power spectrum of the comoving curvature perturbations from the waterfall field in hybrid inflation with tachyonic preheating is very blue: it depends on comoving wavenumber k like $(k/k_*)^3$ (for $k < k_*$) and is negligible on the cosmological scales. Absolute value of the spectrum amplitude at $k \sim k_*$ (as well as the value of k_*) depends on model parameters. In principle, this spectrum at $k \sim k_*$ may be quite substantial, and, in this case, it may be constrained by data of primordial black hole (PBH) and relict gravitational wave (GW) searches.

It is well known that steeply blue spectra of the comoving curvature perturbation are predicted in models with false vacuum inflation, for example in the concrete model where the inflationary potential has a local minimum for a trapping of the field and a high temperature correction for a termination of inflation [11, 12].

Primordial density perturbation spectra with blue tilt (of $(k/k_*)^n$-type) or, more generally, spectra having broad peak features at some k_* value are predicted in two-field models of inflation ending by preheating (going through the parametric resonance) [13] and even in one-field inflation models (in particular, in models with tachyonic preheating after small-field inflation [14, 15]). The characteristic values of k_* (i.e., the k-values of modes which become dominant as a result of tachyonic amplification or parametric resonance) are different in different models. In preheating after chaotic inflation [16, 17] where the perturbations are amplified by parametric resonance, power spectra are peaked at scales $k/aH \gg 1$, whereas in models of small-field inflation the spectra may be peaked around the Hubble scale. In preheating after hybrid inflation, the typical scale of k-values amplified by the tachyonic instability must be sub-Hubble if the phase transition is fast, i.e., if it takes less than a Hubble time [1, 18]. Clearly, the k-value of the

*e-mail: bugaev@pcbai10.inr.ruhep.ru
†e-mail: pklimai@gmail.com

dominantly amplified mode is an important characteristic of a preheating model because large curvature and density perturbations of the Hubble size may result in an abundant production of PBHs and GWs.

In the first stage of tachyonic preheating in models of hybrid inflation the amplification of initial quantum fluctuations of the non-inflaton field is realized due to the classical inflaton rolling or, in a case of the small initial velocity of the inflaton field, due to processes of quantum diffusion [10]. The former case is characterized by the existence of a period of the linear evolution of the non-inflaton field. The evolution in this case can be studied using the cosmological perturbation theory [19–21] or δN approach [22, 23].

In the present paper we want to study in detail the dependence of the primordial curvature perturbations produced by hybrid inflation with tachyonic preheating on parameters of the inflationary potential. We show, in particular, that perturbation amplitudes strongly depend on the mass of the waterfall field m_χ. More exactly, it depends on the relation $|m_\chi^2/H^2|$, where H is a value of the Hubble parameter during inflation. At small values of this relation, $|m_\chi^2/H^2| \sim 1$, the waterfall transition is rather slow, and the expansion of the Universe can not be ignored. Our main aim is to predict concrete values of the perturbation spectrum amplitudes, as well as a form of the k-dependence of the spectrum. So, we preferred to use the results of the numerical (rather that analytical) solution of the equations for the time evolution of the waterfall field. The approximate analytic expression for the power spectrum amplitude, according to which one has, roughly, [7]

$$\mathcal{P}_\zeta \sim \left|\frac{H^2}{m_\chi^2}\right| \cdot \left(\frac{k}{k_*}\right)^3, \qquad k < k_*, \tag{1}$$

were obtained in the limit of the fast waterfall transition, when $|m_\chi^2| \gg H^2$, and can not be used in a whole region of the parameter space.

The plan of the paper is as follows. In Sec. II we calculate the time evolution of the power spectra of the waterfall field perturbations and the spectra at the end of the waterfall. The curvature perturbation spectra from the waterfall, as a function of model parameters, are calculated in Sec. III. In Sec. IV we give estimates for the possibility of PBH production in hybrid inflation model, with taking into account the non-Gaussianity of produced perturbations. Sec. V contains our conclusions.

II. CALCULATION OF WATERFALL FIELD AMPLITUDES

We consider the hybrid inflation model which describes an evolution of the slowly rolling inflaton field ϕ and the waterfall field χ, with the potential [24, 25]

$$V(\phi,\chi) = \left(M^2 - \frac{\sqrt{\lambda}}{2}\chi^2\right)^2 + \frac{1}{2}m^2\phi^2 + \frac{1}{2}\gamma\phi^2\chi^2. \tag{2}$$

The first term in Eq. (2) is a potential for the waterfall field χ with the false vacuum at $\chi = 0$ and true vacuum at $\chi_0^2 = 2M^2/\sqrt{\lambda} \equiv v^2$. The effective mass of the waterfall field in the false vacuum state is given by

$$m_\chi^2(\phi) = \gamma\left(\phi^2 - \phi_c^2\right), \quad \phi_c^2 \equiv \frac{2M^2\sqrt{\lambda}}{\gamma}. \tag{3}$$

At $\phi^2 > \phi_c^2$ the false vacuum is stable, while at $\phi^2 < \phi_c^2$ the effective mass-squared of χ becomes negative, and there is a tachyonic instability leading to a rapid growth of χ-modes and eventually to an end of the inflationary expansion.

The evolution equations for the fields are given by

$$\ddot{\phi} + 3H\dot{\phi} = -\phi(m^2 + \gamma\chi^2), \tag{4}$$

$$\ddot{\chi} + 3H\dot{\chi} - \nabla^2\chi = (2\sqrt{2}M^2 - \gamma\phi^2 - \lambda\chi^2)\chi. \tag{5}$$

Here, we ignore the spatial gradient term in the equation for ϕ. Before the waterfall transition, i.e., at $\phi^2 > \phi_c^2$, the waterfall field is trapped at $\chi = 0$, so we can consider Eq. (5) as an equation for the vacuum fluctuation $\delta\chi$.

One should note that, as we will see below, the typical scale of the fluctuations amplified during the waterfall transition is of the order of the Hubble scale, or larger. In such a case, the back-reaction effects (due to perturbations of metric) may be non-negligible. To minimize the back-reaction effects, we will work in the vacuum-dominated regime, i.e., we assume that the vacuum energy M^4 dominates, so that the Hubble parameter is effectively a constant,

$$H^2 = H_c^2 = \frac{M^4}{3M_P^2}. \tag{6}$$

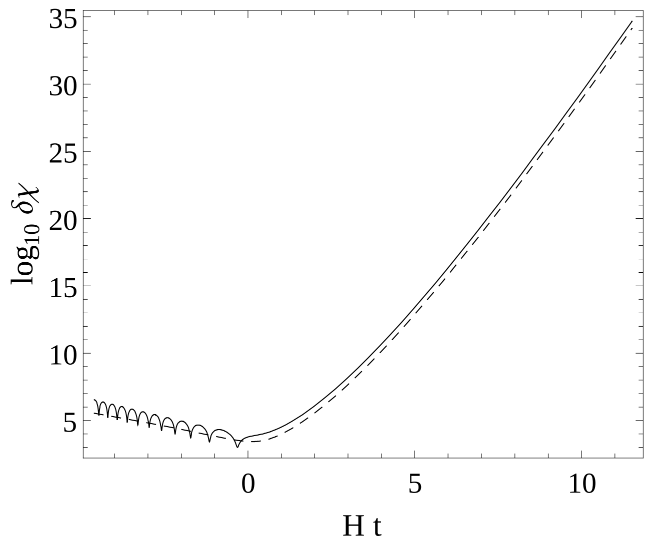

FIG. 1: The numerically calculated dependence of $\delta\chi_k$ on time for two values of k: $k = 0.01H_c$ (solid curve) and $k = H_c$ (dashed curve). Other parameters used for the calculation are: $\beta = 100$, $r = 0.1$, $H_c = 10^{11}$ GeV, $\phi_c = 0.1M_P$. For this set of parameters, the waterfall ends near $Ht \approx 3.5$, but we proceed the curves further just to show the asymptotic behavior.

Besides, we consider only the case of small $\dot{\phi}$, satisfying the condition

$$\frac{\dot{\phi}}{H\delta\phi} \ll 1. \tag{7}$$

As for Eq. (5), the back-reaction effects are small because the unperturbed value of $\langle\chi\rangle$ is equal to zero [1].

The solution of Eq. (4) is (for $t > t_c$, t_c is the critical point when the tachyonic instability begins)

$$\phi = \phi_c e^{-rH_c(t-t_c)}, \quad r = \frac{3}{2} - \sqrt{\frac{9}{4} - \frac{m^2}{H_c^2}}. \tag{8}$$

The scale factor a is normalized to 1 at the time of the beginning of the waterfall (at $t = t_c = 0$), so

$$a = e^{H_c t}. \tag{9}$$

The conformal time in this case is

$$\eta = -\frac{1}{H_c}e^{-H_c t} = -\frac{1}{aH_c}, \tag{10}$$

corresponding to the de Sitter expansion.

From Eq. (5), one obtains the equation for Fourier modes of $\delta\chi$:

$$\delta\ddot{\chi}_k + 3H\delta\dot{\chi}_k + \left(\frac{k^2}{a^2} - \beta H_c^2 + \gamma\phi^2\right)\delta\chi_k = 0. \tag{11}$$

Here, the parameter β is given by the relation

$$\beta = 2\sqrt{\lambda}\frac{M^2}{H_c^2}. \tag{12}$$

Substituting the solution for ϕ in Eq. (11) and introducing the new variable, $u = a\delta\chi$, one obtains the equation

$$u_k'' + (k^2 + \mu^2(\eta))u_k = 0, \quad \mu^2(\eta) = \frac{\beta(|\eta H_c|^{2r} - 1) - 2}{\eta^2}. \tag{13}$$

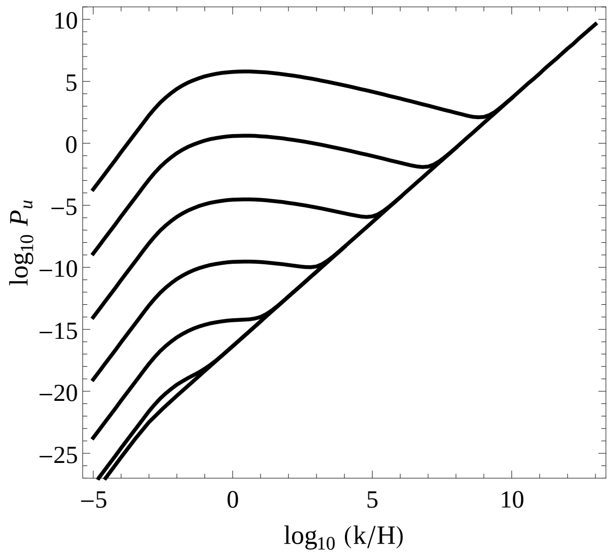

FIG. 2: The numerically calculated spectra $\mathcal{P}_u(k)$ at different moments of time, for $\beta = 1$, $r = 0.1$, $H_c = 10^{11}$ GeV, $\phi_c = 3 \times 10^{-6} M_P$. From bottom to top, $-\eta H = 10^3, 10^1, 10^{-1}, 10^{-3}, 10^{-5}, 10^{-7}, 10^{-9}$ (the waterfall ends near $-\eta H = 10^{-9}$).

Here, primes denote the derivative with respect to conformal time η. The normalization at early times, when $k \gg \mu$, is $u = \frac{1}{\sqrt{2k}} e^{-ik\eta}$. The definition of the power spectrum of u, as usual, is

$$\mathcal{P}_u = \frac{k^3}{2\pi^2} P_u = \frac{k^3}{2\pi^2} |u_k|^2. \tag{14}$$

We show some results of numerical calculations in Figs. 1-3. In Fig. 1 we show how χ_k depends on time for two different values of k ($k = H$ and $k \ll H$). It is seen that time evolution of both modes after the waterfall is almost the same. Following [5] we assume that the growth era ends when the last term in right-hand side of Eq. (4) becomes equal to the preceding one, i.e, when

$$\langle \chi^2 \rangle = \frac{m^2}{\gamma} \equiv \chi_{nl}^2. \tag{15}$$

The asymptotic growth law of k-modes of the waterfall field is approximately [3]

$$\chi \sim e^{sHt}, \quad s = \sqrt{\frac{9}{4} + \beta} - \frac{3}{2}. \tag{16}$$

It follows from Eq. (16) that at large β the asymptotics of χ is $e^{\sqrt{\beta} Ht}$, and the time scale of a period of the tachyonic instability is much less than a Hubble time.

The typical example of the calculation of the power spectrum of u is shown in Fig. 2. This Figure is similar with Fig. 3 of [3], where analogous quantities for the case $\beta = 100, r = 0.1$ were shown. It is seen from our Fig. 2 that even for the case $\beta = 1$ the waterfall is still effective, however it is much slower (it takes ~ 20 e-folds for $\beta = 1$ while in the case of $\beta = 100$ the number of e-folds is ~ 3.5).

Fig. 3 shows the form of $\mathcal{P}_{\delta\chi}(k)$ at the moment of the end of the waterfall (determined by Eq. (15)), for several parameter sets. Note also, that we impose an artificial cutoff of large-k modes in our numerical calculation, which corresponds to considering only the waterfall field modes that already became classical at the beginning of the waterfall. Technically, the cutoff is imposed at the local minimum of $\mathcal{P}_{\delta\chi}(k)$-curve.

After a calculation of the power spectrum of $\delta\chi$, we calculate the spectrum $P_{\delta\chi^2}(k)$ at the end of the waterfall by the formula followed from the convolution theorem [26]:

$$P_{\chi^2}(k) = \frac{2}{(2\pi)^3} \int d^3k' P_\chi(k') P_\chi(|\vec{k} - \vec{k}'|). \tag{17}$$

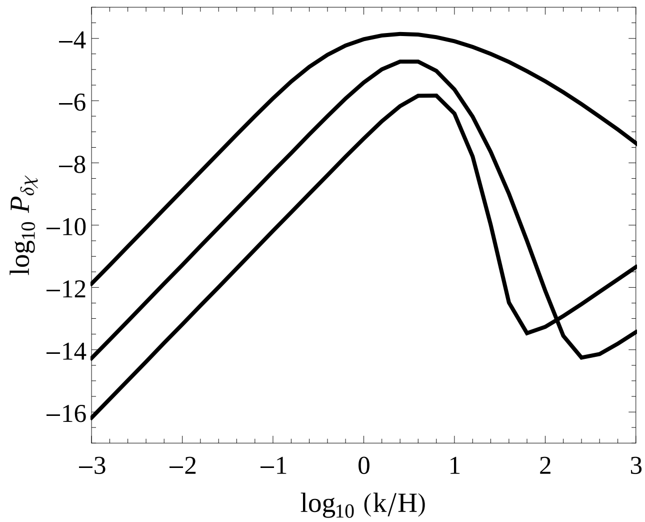

FIG. 3: The numerically calculated spectra $\mathcal{P}_{\delta\chi}(k)$ at the moment of the end of the waterfall. For all cases, $r = 0.1$, $H_c = 10^{11}$ GeV, $\phi_c = 0.1 M_P$. From bottom to top, $\beta = 1500, 100, 7$.

III. CURVATURE PERTURBATION SPECTRUM

The main equation for a calculation of the primordial curvature perturbation (on uniform density hypersurfaces) is [27]

$$\zeta = - \int dt \frac{H \delta p_{nad}}{p + \rho}, \tag{18}$$

where the non-adiabatic pressure perturbation is $\delta p_{nad} = \delta p - c_s^2 \delta \rho$ and the adiabatic sound speed is $c_s^2 = \dot{p}/\dot{\rho}$. The formula (18) follows from the "separated universes" picture where, after smoothing over sufficiently large scales, the universe becomes similar to an unperturbed FRW cosmology. In our case, one has

$$p + \rho = \dot{\phi}^2 + \langle \dot{\chi}^2 \rangle, \tag{19}$$

and

$$\delta p_{nad} = \delta p_\chi - \frac{\dot{p}}{\dot{\rho}} \, \delta \rho_\chi \tag{20}$$

($p = p_\phi + \langle p_\chi \rangle$; $\rho = \rho_\phi + \langle \rho_\chi \rangle$).

For p_χ and ρ_χ, neglecting spatial gradients, we can write (χ and $\dot{\chi}$ are functions of both time and coordinates):

$$p_\chi = - \frac{m_\chi^2(t)}{2} \chi^2 + \frac{1}{2} \dot{\chi}^2, \tag{21}$$

$$\rho_\chi = \frac{m_\chi^2(t)}{2} \chi^2 + \frac{1}{2} \dot{\chi}^2 \tag{22}$$

(where, for brevity, $m_\chi^2\,(\phi(t)) \equiv m_\chi^2(t)$).

The possibility of ignoring of spatial gradient terms in expressions for ρ_χ and p_χ is discussed in [1, 7]. It was shown there that there are two sufficient conditions for such a possibility: *i)* the exponential growth of the fluctuations is dominated by the modes with typical momentum k_*, and *ii)* the χ-field is heavy, i.e., $|m_\chi^2| \gtrsim H^2$, or $\beta \gtrsim 1$.

If a time behavior of $\chi(\vec{x}, t) \equiv \chi(t)$ is known, $\chi(t) = C f(t)$ (where $f(t)$ is an arbitrarily normalized function giving time behavior of $\chi(t)$; it is seen, in particular, from Fig. 1, that time evolution of different modes of χ is almost the same), then

$$\dot{\chi}(t) = C \dot{f}(t) = \chi(t) \frac{\dot{f}(t)}{f(t)}, \tag{23}$$

so we can write

$$\delta p_\chi = \frac{1}{2}\left[-m_\chi^2(t) + \left(\frac{\dot{f}(t)}{f(t)}\right)^2\right]\delta\chi^2, \tag{24}$$

$$\delta \rho_\chi = \frac{1}{2}\left[m_\chi^2(t) + \left(\frac{\dot{f}(t)}{f(t)}\right)^2\right]\delta\chi^2, \tag{25}$$

and, because $\chi(t) = Cf(t)$,

$$\langle\chi^2(t)\rangle = \chi_{nl}^2 \frac{f^2(t)}{f^2(t_{end})}, \tag{26}$$

$$\langle\dot{\chi}^2(t)\rangle = \chi_{nl}^2 \frac{\dot{f}^2(t)}{f^2(t_{end})}. \tag{27}$$

Finally, for the average values, one has

$$\langle p_\chi\rangle = \frac{1}{2}\left[-m_\chi^2(t) + \left(\frac{\dot{f}(t)}{f(t)}\right)^2\right]\left(\frac{f(t)}{f(t_{end})}\right)^2\chi_{nl}^2, \tag{28}$$

$$\langle \rho_\chi\rangle = \frac{1}{2}\left[m_\chi^2(t) + \left(\frac{\dot{f}(t)}{f(t)}\right)^2\right]\left(\frac{f(t)}{f(t_{end})}\right)^2\chi_{nl}^2. \tag{29}$$

The values of p_ϕ and ρ_ϕ are

$$p_\phi = -V(\phi) + \frac{1}{2}\dot{\phi}^2, \quad \rho_\phi = V(\phi) + \frac{1}{2}\dot{\phi}^2, \tag{30}$$

where, for our case, $V(\phi) = \frac{1}{2}m^2\phi^2$.

For the curvature perturbation, we have the integral

$$\zeta = -\int \frac{H_c dt}{\dot{\phi}^2 + \langle\dot{\chi}^2\rangle}\frac{\delta\chi^2(t)}{2}\left[-m_\chi^2(t) + \left(\frac{\dot{f}(t)}{f(t)}\right)^2 - \frac{\dot{p}}{\dot{\rho}}\left(m_\chi^2(t) + \left(\frac{\dot{f}(t)}{f(t)}\right)^2\right)\right]. \tag{31}$$

The relation between curvature perturbation and χ^2-spectra is

$$\mathcal{P}_\zeta = A^2\mathcal{P}_{\delta\chi^2}(t_{end}), \tag{32}$$

where the value of the spectrum in the right-hand side is calculated at a time of the end of the waterfall, t_{end}, and A is to be determined. The values of χ^2 at different times are related by

$$\chi^2(t) = \chi^2(t_{end})\left(\frac{f(t)}{f(t_{end})}\right)^2, \tag{33}$$

so we can extract the value of A,

$$A = \int_0^{t_{end}} \frac{H_c dt}{\dot{\phi}^2 + \langle\dot{\chi}^2\rangle}\left(\frac{f(t)}{f(t_{end})}\right)^2\frac{1}{2}\left[-m_\chi^2(t) + \left(\frac{\dot{f}(t)}{f(t)}\right)^2 - \frac{\dot{p}}{\dot{\rho}}\left(m_\chi^2(t) + \left(\frac{\dot{f}(t)}{f(t)}\right)^2\right)\right]. \tag{34}$$

We show results of the calculation of $\mathcal{P}_\zeta(k)$ in Fig. 4. It is seen that the spectrum can reach rather large values (of order of 1) for the case of $\beta \sim 1$ (if r is in a broad interval, say, $0.1 \div 0.001$).

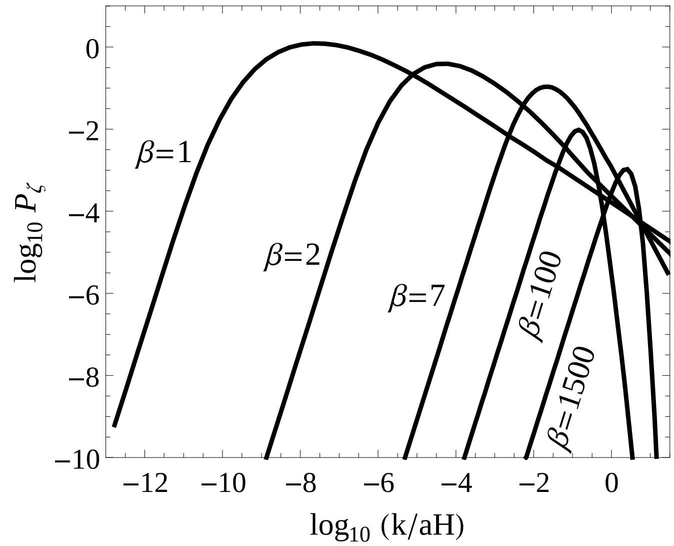

FIG. 4: The numerically calculated spectra $\mathcal{P}_\zeta(k)$ at the moment of the end of the waterfall. Parameters used for the calculation are: $r = 0.1$, $H_c = 10^{11}$ GeV (all curves); $\phi_c = 3 \times 10^{-6} M_P$ (for $\beta = 1, 2, 7$); $\phi_c = 0.1 M_P$ (for $\beta = 100, 1500$).

In Fig. 5 we show the model parameter regions that lead to rather large values of $\mathcal{P}_\zeta$. We also show, on the same Figure, the parameter region where waterfall is not effective (classical regime is not reached) and boundary of $\phi_c = 1$ (in units of Planck mass M_P).

At the end of this section, we numerate the constraints on the parameter space which follow from the assumptions used for an obtaining of the main results.

1. Slow roll of the inflaton field:

$$m^2 \ll H_c^2. \tag{35}$$

2. False vacuum dominance:

$$M^4 \gg \frac{1}{2} m^2 \phi_c^2. \tag{36}$$

3. Small ϕ-condition (for justifying of the omission of high powers of ϕ in the inflaton potential):

$$\phi_c \ll M_P. \tag{37}$$

4. Small effects from back-reaction:

$$\frac{\dot{\phi}}{H \delta\phi} \ll 1. \tag{38}$$

If $\delta\phi \sim H_c/2\pi$, it leads to $2\pi r^2/\sqrt{\gamma} \ll 1$.

5. Condition for $\delta\chi_k$ to be classical field [1]

$$\sqrt{\gamma} \ll \frac{1}{\sqrt{\beta}}. \tag{39}$$

6. Condition for a dominance of the scenario with the inflaton's classical rolling [18]:

$$\dot{\phi}_c > \gamma \lambda v^2, \quad \text{or} \quad \gamma^{3/2} < \sqrt{r}. \tag{40}$$

IV. PBH PRODUCTION FROM NON-GAUSSIAN PERTURBATIONS

A production of PBHs during reheating process had been considered in works [13, 14, 28–30]. The classical PBH formation criterion in the radiation-dominated epoch is [31]

$$\delta > \delta_c \approx 1/3, \tag{41}$$

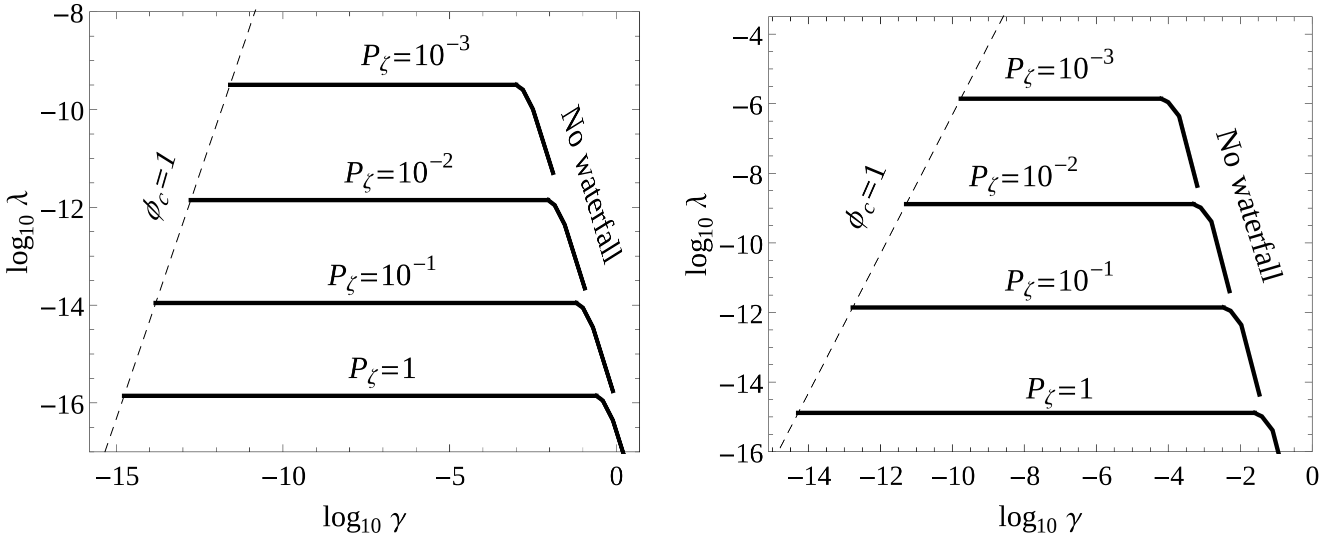

FIG. 5: The allowed ranges for the values of γ and λ and the corresponding maximum values of $\mathcal{P}_\zeta(k)$ that are reached. Left panel: $r = 0.1$ ($m \approx 0.5H_c$). Right panel: $r = 0.001$ ($m \approx 0.05H_c$). For both panels, $H_c = 10^{11}$ GeV.

where δ is the smoothed density contrast at horizon crossing. The Fourier component of the comoving density perturbation δ is related to the Fourier component of the Bardeen potential Ψ as

$$\delta_k = -\frac{2}{3}\left(\frac{k}{aH}\right)^2 \Psi_k. \tag{42}$$

For modes in a super-horizon regime, $\Psi_k \approx -(2/3)\mathcal{R}_k \approx -(2/3)\zeta_k$, so (41) can be translated to a limiting value of the curvature perturbation [32], which is

$$\zeta_c \approx 0.7. \tag{43}$$

It is seen from (31) that the curvature perturbation generated by waterwall field has a negative sign, so, naively, the threshold (43) can't be reached. However, the perturbations must be considered with respect to the average value, so

$$\zeta \to \zeta_0 = \zeta - \langle\zeta\rangle, \tag{44}$$

and the condition for individual PBH formation is $\zeta_0 \gtrsim \zeta_c$, while PBHs will exceed the currently available limits on their average abundance already for $|\langle\zeta\rangle|$ only slightly exceeding ζ_c (i.e., $|\langle\zeta\rangle| - \zeta_c \ll 1$) [7], so, practically, the PBH constraint on ζ is just $|\langle\zeta\rangle| < \zeta_c$.

For the distribution of ζ_0 we may write

$$\zeta_0 = -(g^2 - \langle g^2\rangle), \tag{45}$$

where g is gaussian (in our case, $g \sim \delta\chi$), and for the average of ζ_0^2, using known properties of Gaussian distributions,

$$\langle\zeta_0^2\rangle = 2\langle g^2\rangle^2 = 2|\langle\zeta\rangle|^2, \tag{46}$$

so, in terms of $\langle\zeta_0^2\rangle$ the significant PBH formation will happen if

$$\langle\zeta_0^2\rangle = \int \mathcal{P}_\zeta(k)\frac{dk}{k} \gtrsim 2\zeta_c^2 \approx 1. \tag{47}$$

In case of $\mathcal{P}_\zeta$-spectra shown in Fig. 4, the curve corresponding to $\beta = 2$ is close to the bound (47) while the curve for $\beta = 1$ has $\langle\zeta^2\rangle \approx 7$ which makes that set of parameters forbidden by the PBH formation constraint.

The mass of the PBHs produced from curvature perturbation spectra presented in Fig. 4 can be estimated as follows. The horizon mass at the end of inflation is

$$M_i \approx (H_c^{-1})^3\rho = \frac{3M_P^2}{H_c} \sim 10^2 \text{ g}, \tag{48}$$

and using a well-known dependence for the horizon mass corresponding to fluctuation having wave number k, $M_h \sim k^{-2}$ (see, e.g., [33]), we have

$$M_{BH} \approx M_h \approx M_i \left(\frac{a(t_{end}) H_c}{k} \right)^2 . \quad (49)$$

For the case of Fig. 4, curve for $\beta = 1$ corresponds to $M_{BH} \sim 10^{19}$ g (the mass range of non-evaporating PBHs that can constitute dark matter) while $\beta = 2$ corresponds to $M_{BH} \sim 10^{13}$ g (such PBHs have already evaporated, but the products of their evaporation can be, in principle, observable).

V. CONCLUSIONS

We carried out numerical calculations of a contribution of the waterfall field to the primordial curvature perturbation (on uniform density hypersurfaces) ζ, which is produced during waterfall transition in hybrid inflation scenario. The calculation is performed for a broad interval of values of the model parameters.

We did not consider the contribution to ζ from inflaton rolling, which is dominant at cosmological scales. One should note that the simple quadratic inflationary potential used in the present paper can be easily corrected (see, e.g., [34]) to give a red-tilted spectrum at cosmological scales (converting, e.g., the original hybrid inflation model to a hilltop model [35, 36]), without any modification of our predictions for small scales.

Main results of the paper are shown in Figs. 4, 5. One can see from the Fig. 4 that peak amplitudes of $\mathcal{P}_\zeta$ strongly depend on the value of β (curiously, $\mathcal{P}_\zeta \sim 1$ corresponds to $\beta \sim 1$ in a broad interval of γ and r). The peak values, k_*, for small β are far beyond horizon, so, the smoothing over the horizon size will not decrease the peak values of the smoothed spectrum. Furthermore, the spectrum near peak remains strongly non-Gaussian after the smoothing. Our calculations based on the quadratic inflaton potential show that for $\beta \lesssim 100$ and in the broad interval of r the peak value k_* can be estimated by the simple relation:

$$\frac{k_*}{aH} \sim e^{-N}, \quad (50)$$

where N is the number of folds during the waterfall transition.

We conclude that the strong growth of amplitudes of the curvature perturbation spectrum at $\beta \to 1$, which had been anticipated in pioneering works [37, 38], really takes place. However, the condition which is very often used as a constraint, that the bare mass-squared of the χ-field, $-m_\chi^2 = 2\sqrt{\lambda} M^2$, must be *much larger* that H^2 (the so-called "waterfall condition" [39]) seems to be too restrictive. Our results show that only at $-m_\chi^2 \approx H^2$ the amplitute of the curvature spectrum $\mathcal{P}_\zeta$ becomes close to one, i.e., enters into a region that can be constrained by PBH data. It would be very interesting to analyze the corresponding constraints following from data of relict GW searches (see, e.g., [18, 40, 41]).

[1] D. H. Lyth, arXiv:1005.2461 [astro-ph.CO].
[2] J. O. Gong and M. Sasaki, JCAP **1103**, 028 (2011) [arXiv:1010.3405 [astro-ph.CO]].
[3] J. Fonseca, M. Sasaki and D. Wands, JCAP **1009**, 012 (2010) [arXiv:1005.4053 [astro-ph.CO]].
[4] A. A. Abolhasani, H. Firouzjahi, Phys. Rev. **D83**, 063513 (2011) [arXiv:1005.2934 [hep-th]].
[5] D. H. Lyth, arXiv:1012.4617 [astro-ph.CO].
[6] A. A. Abolhasani, H. Firouzjahi, M. Sasaki, arXiv:1106.6315 [astro-ph.CO].
[7] D. H. Lyth, arXiv:1107.1681 [astro-ph.CO].
[8] R. Kallosh, Lect. Notes Phys. **738**, 119-156 (2008) [hep-th/0702059 [HEP-TH]].
[9] R. Kallosh, A. D. Linde, JCAP **0310**, 008 (2003) [hep-th/0306058].
[10] G. N. Felder, J. Garcia-Bellido, P. B. Greene, L. Kofman, A. D. Linde, I. Tkachev, Phys. Rev. Lett. **87**, 011601 (2001) [hep-ph/0012142].
[11] L. Pilo, A. Riotto and A. Zaffaroni, Phys. Rev. Lett. **92**, 201303 (2004) [arXiv:astro-ph/0401302].
[12] J. -O. Gong, M. Sasaki, JCAP **0901**, 001 (2009) [arXiv:0804.4488 [astro-ph]].
[13] T. Suyama, T. Tanaka, B. Bassett and H. Kudoh, Phys. Rev. D **71**, 063507 (2005) [arXiv:hep-ph/0410247].
[14] T. Suyama, T. Tanaka, B. Bassett and H. Kudoh, JCAP **0604**, 001 (2006) [arXiv:hep-ph/0601108].
[15] P. Brax, J. -F. Dufaux, S. Mariadassou, Phys. Rev. **D83**, 103510 (2011) [arXiv:1012.4656 [hep-th]].
[16] L. Kofman, A. D. Linde and A. A. Starobinsky, Phys. Rev. Lett. **73**, 3195 (1994) [arXiv:hep-th/9405187].
[17] L. Kofman, A. D. Linde and A. A. Starobinsky, Phys. Rev. D **56**, 3258 (1997) [arXiv:hep-ph/9704452].

[18] J. F. Dufaux, G. N. Felder, L. Kofman, O. Navros, JCAP **0903**, 001 (2009) [arXiv:0812.2917 [astro-ph]].
[19] T. Asaka, W. Buchmuller, L. Covi, Phys. Lett. **B510**, 271-276 (2001) [hep-ph/0104037].
[20] E. J. Copeland, S. Pascoli and A. Rajantie, Phys. Rev. D **65**, 103517 (2002) [arXiv:hep-ph/0202031].
[21] J. Garcia-Bellido, M. Garcia Perez and A. Gonzalez-Arroyo, Phys. Rev. D **67**, 103501 (2003) [arXiv:hep-ph/0208228].
[22] M. Sasaki and E. D. Stewart, Prog. Theor. Phys. **95** (1996) 71 [arXiv:astro-ph/9507001].
[23] D. H. Lyth, K. A. Malik, M. Sasaki, JCAP **0505**, 004 (2005) [astro-ph/0411220].
[24] A. D. Linde, Phys. Lett. B **259**, 38 (1991).
[25] A. D. Linde, Phys. Rev. **D49**, 748-754 (1994) [astro-ph/9307002].
[26] D. H. Lyth, Phys. Rev. **D45**, 3394-3404 (1992).
[27] D. Wands, K. A. Malik, D. H. Lyth and A. R. Liddle, Phys. Rev. D **62**, 043527 (2000) [arXiv:astro-ph/0003278].
[28] A. M. Green, K. A. Malik, Phys. Rev. **D64**, 021301 (2001) [hep-ph/0008113].
[29] B. A. Bassett, S. Tsujikawa, Phys. Rev. **D63**, 123503 (2001) [hep-ph/0008328].
[30] F. Finelli, S. Khlebnikov, Phys. Lett. **B504**, 309-313 (2001) [hep-ph/0009093].
[31] B. J. Carr, S. W. Hawking, Mon. Not. Roy. Astron. Soc. **168**, 399-415 (1974).
[32] J. C. Hidalgo, arXiv:0708.3875 [astro-ph].
[33] E. Bugaev and P. Klimai, Phys. Rev. D **78**, 063515 (2008) [arXiv:0806.4541 [astro-ph]].
[34] M. U. Rehman, Q. Shafi, J. R. Wickman, Phys. Rev. **D79**, 103503 (2009) [arXiv:0901.4345 [hep-ph]].
[35] L. Boubekeur, D. .H. Lyth, JCAP **0507**, 010 (2005) [hep-ph/0502047].
[36] K. Kohri, C. -M. Lin, D. H. Lyth, JCAP **0712**, 004 (2007) [arXiv:0707.3826 [hep-ph]].
[37] L. Randall, M. Soljacic, A. H. Guth, Nucl. Phys. **B472**, 377-408 (1996) [hep-ph/9512439].
[38] J. Garcia-Bellido, A. D. Linde, D. Wands, Phys. Rev. **D54**, 6040-6058 (1996) [astro-ph/9605094].
[39] E. J. Copeland, A. R. Liddle, D. H. Lyth, E. D. Stewart, D. Wands, Phys. Rev. **D49**, 6410-6433 (1994) [astro-ph/9401011].
[40] E. Bugaev, P. Klimai, Phys. Rev. **D83**, 083521 (2011) [arXiv:1012.4697 [astro-ph.CO]].
[41] M. Giovannini, Phys. Rev. D **82**, 083523 (2010) [arXiv:1008.1164 [astro-ph.CO]].